Manganese−Chalcocarbonyl Bond Strengths from Threshold Photoelectron Photoion Coincidence Spectroscopy

Ágnes Révész,† Csaba István Pongor,† Andras Bodi,† Bálint Sztáray,*,† and Tomas Baer‡

Institute of Chemistry, Eötvös Loránd University, Budapest, Hungary, and Department of Chemistry, University of North Carolina, Chapel Hill, North Carolina

Received May 2, 2006

The dissociation kinetics of $CpMn(CO)_2CX$ (X = S, Se) complexes have been investigated by threshold photoelectron photoion coincidence (TPEPICO) spectroscopy. Energy-selected $CpMn(CO)_2CX^+$ ions sequentially lose the two carbonyl and chalcocarbonyl ligands upon photoionization. The resulting asymmetric time-of-flight peak shapes and breakdown diagrams were simulated, and the following 0 K appearance energies were determined for the fragment ions: $CpMn(CO)CS^+$, 8.79 ± 0.05 eV; $CpMnCS^+$, 9.42 ± 0.05 eV; $CpMn^+$, 11.53 ± 0.05 eV; $CpMn(CO)CSe^+$, 8.70 ± 0.05 eV; $CpMnCSe^+$, 9.39 ± 0.05 eV; and $CpMn^+$, 12.05 ± 0.05 eV. These values, combined with the adiabatic ionization energies, yield Mn−CO bond energies in $CpMn(CO)_2CX^+$ (X = S, Se) and $CpMn(CO)CX^+$ (1.20 ± 0.06, 0.63 ± 0.07 eV and 1.08 ± 0.06, 0.72 ± 0.07 eV, respectively) and Mn−CX bond energies in $CpMnCX^+$ (X = S, Se, 2.12 ± 0.07 and 2.66 ± 0.07 eV, respectively).The 0 K heats of formation of the neutral and ionic species were determined using the heats of formation of the dissociation products, $CpMn^+$, CO, and CX. Thus, it became possible to obtain Mn−CX bond energies in both parent ions and both first daughter ions. Room-temperature gaseous heats of formation are also given using ab initio thermal enthalpies. On average, in the ions, the Mn−CX bond energies are larger than Mn−CO bond energies by 1.04 eV (X = S) and 1.61 eV (X = Se). Using the appearance energy of $CpMn^+$ in the earlier TPEPICO studies of $CpMn(CO)_3$, the carbonyl → calcocarbonyl substitution heats were determined for the neutral complexes.

Introduction

Transition metal complexes are widely used as catalysts or chemical vapor deposition precursors. Transition metal carbonyls, which are used in catalytic reactions as well as chemical vapor deposition, are an especially interesting and useful group of complexes. The usual starting step for the formation of the catalytically active, coordinatively unsaturated species is the metal−carbonyl bond rupture. Therefore, the thermochemistry and especially the transition metal carbonyl bond energies are of great importance in catalyst design. In the past few years, our group has investigated the gas-phase thermochemistry of a number of organometallic complexes, such as $CpMn(CO)_3$,[1] $CpCo(CO)_2$,[2,3] $C_6H_6Cr(CO)_3$,[4] Cp_2Mn,[5] $(C_6H_6)_2Cr$,[6] $Co(CO)_3NO$[7] (Cp = C_5H_5), and their substituted analogues.

Carbon monosulfide, CS, and carbon monoselenide, CSe, are unstable in contrast with carbon monoxide, but they can be stabilized as ligands in transition metal complexes. The properties (stability, reactivity) of several thiocarbonyl[8−10] complexes compared to the carbonyl analogues suggest the $[M−CS]^+$ bond is stronger than the $[M−CO]^+$. Several thiocarbonyl complexes have been studied by electron ionization (EI) mass spectrometric experiments,[11−16] which showed that the thiocarbonyl (CS) ligand forms a stronger bond to the transition metal center than the carbonyl ligand. By comparing $M(CO)_6$ molecules with the analogous $M(CO)_5CS$ (M = Cr, Mo, W)[11] complexes, it was found that the $[M - CS]^+$ dissociation energy is 1.5−2.0 eV larger than the $[M - CO]^+$ dissociation energy. The $CpMn(CO)_3$ and $CpMn(CO)_2CS$ complexes have also been studied,[14] and the $[Mn - CO]^+$ and $[Mn - CS]^+$ bond energies were found to be 2.39 and 3.00 eV, respectively. Similarly, an electron ionization mass spectrometric study of $CH_3C_5H_4Mn(CO)_2CS$[14] indicated that the derived $[Mn−CO]^+$ and $[Mn−CS]^+$ bond energies are 2.20 and 3.05 eV, respectively. However, due to the neglect of the thermal energy distribution of the sample and the low-energy resolution of the EI experiment, these values may be in significant error. Furthermore, the slow dissociation dynamics were also neglected in the data analysis. The gas-phase reactivities of transition metal sulfides (MS^+, M = Sc,

* Corresponding author. E-mail: szb@elte.hu.
† Eötvös Loránd University.
‡ University of North Carolina.

(1) Li, Y.; Sztáray, B.; Baer, T. *J. Am. Chem. Soc.* **2001**, *123*, 9388.
(2) Sztáray, B.; Baer, T. *J. Am. Chem. Soc.* **2000**, *122*, 9219.
(3) Sztáray, B.; Szepes, L.; Baer, T. *J. Phys. Chem. A* **2003**, *107*, 9486.
(4) Li, Y.; McGrady, J. E.; Baer, T. *J. Am. Chem. Soc.* **2002**, *124*, 4487.
(5) Li, Y.; Sztáray, B.; Baer, T. *J. Am. Chem. Soc.* **2002**, *124*, 5843.
(6) Li, Y.; Baer, T. *J. Phys. Chem.* **2002**, *106*, 9820.
(7) Sztáray, B.; Baer, T. *J. Phys. Chem. A* **2002**, *106*, 8046.
(8) Mansuy, D.; Battioni, J. P.; Chottard, J. C. *J. Am. Chem. Soc.* **1978**, *100* (13), 4311.
(9) Braunstein, P; Knorr, M.; Villaroya, E.; De Cian, A.; Fischer, J. *Organometallics* **1991**, *10* (10), 3714.
(10) Busetto, L.; Palazzi, A. *Inorg. Chim. Acta* **1976**, *19* (3), 233.
(11) Michels, G. D.; Flesch, G. D.; Svec, H. J. *Inorg. Chem.* **1980**, *19*, 479.
(12) Simonneaux, G.; Jaouen, G.; Dabard, R.; Guenot, P. *J. Organomet. Chem.* **1977**, *132*, 231.
(13) Efraty, A.; Liebman, D.; Huang, M. H. A.; Weston, C. A.; Angelici, R. J. *Inorg. Chem.* **1978**, *17*, 2831.
(14) Efraty, A.; Huang, M. H. A.; Weston, C. A. *Inorg. Chem.* **1975**, *14*, 2796.
(15) Efraty, A.; Liebman, D.; Huang, M. H. A.; Weston, C. A. *Inorg. Chim. Acta* **1980**, *39*, 105.
(16) Efraty, A.; Huang, M. H. A. *Inorg. Chem.* **1980**, *19*, 2296.

10.1021/om060379j CCC: $33.50
Publication on Web 11/15/2006

Ti,[17] V, Mo, Fe,[18] Y, Zr, Nb[19]) were investigated with guided-ion beam and Fourier transform ion cyclotron resonance mass spectrometry. These measurements provided values for $[M-CS^+]$ dissociation energies. Quantum chemical calculations also indicate stronger $M-CS^+$ bonds.[20−22] There are fewer data on the thermochemistry and gas-phase ion energetics of selenocarbonyl complexes and their fragments. IR and Raman experiments on $Cr(CO)_5CSe$ and $MeO_2C(C_6H_5)Cr(CO)_2CSe$ suggested that the Cr−CSe bond is stronger than the Cr−CS bond.[23]

$CpMn(CO)_2CS$ and $CpMn(CO)_2CSe$, which are air-sensitive, yellow, crystalline solids, have been studied by ^{13}C NMR[24,25] and mass spectrometry.[14,26] Several IR experiments were carried out on the thiocarbonyl complex.[27−29] The first He I photoelectron spectrum (PES) of $CpMn(CO)_2CS$ was taken by Lichtenberger and co-workers.[30] Recently, we have carried out a He I and He II PES study of this compound and, with the aid of quantum mechanical calculations, proposed a new ordering of the molecular energy levels and, thus, a new assignment for the PE spectrum.[31]

In the present work, energy-selected $CpMn(CO)_2CS^+$ and $CpMn(CO)_2CSe^+$ ions have been prepared and their gas-phase unimolecular dissociation kinetics have been studied with threshold photoelectron photoion coincidence spectroscopy (TPEPICO). The experimental results, along with a statistical (RRKM) analysis of the dissociation rates and energetics, provide bond energies of the ionic species. From the known heat of formation of the final ionic product, $CpMn^+$, it is possible to determine the heats of formation of both the molecular ion and the various fragment ions, as well as that of the neutral molecule. Combining the heats of formation of the neutral chalcocarbonyl-substituted molecules with the known heat of formation of $CpMn(CO)_3$[1] leads to substitution enthalpies for the $CpMn(CO)_3 + CX \rightarrow CpMn(CO)_2CX + CO$ reactions. These data refer to relative bond strengths in the neutral rather than ionic complexes and, therefore, are of greater importance to organometallic chemists.

Experimental Section

Experimental Approach. The syntheses of the $CpMn(CO)_2CX$ (X = S, Se) complexes were carried out under an inert atmosphere by the following procedure:[32,33]

$$CpMn(CO)_3 \xrightarrow{cis-\text{cyclooctene, UV}} CpMn(CO)_2(cis\text{-cyclooctene}) + CO$$

$$CpMn(CO)_2(\text{cyclooctene}) \xrightarrow{CS_2,\ P(Ph)_3} CpMn(CO)_2CS + (Ph)_3PS + C_8H_{14}$$

$$CpMn(CO)_3 \xrightarrow{\text{THF, UV}} CpMn(CO)_2(THF) + CO$$

$$CpMn(CO)_2(THF) \xrightarrow{CSe_2,\ P(Ph)_3} CpMn(CO)_2CSe + (Ph)_3PSe + THF$$

The samples were purified by in-vacuo sublimation and characterized by their mass and IR spectra.

The TPEPICO apparatus has been described in detail previously.[34,35] Briefly, the sample was leaked into the experimental chamber through a 2.5 cm long and 1.0 mm wide inlet. It was necessary to heat the solid sample to 50 °C ($CpMn(CO)_2CS$) and 55 °C ($CpMn(CO)_2CSe$) to obtain a sufficient vapor pressure. The sample molecules were ionized with vacuum ultraviolet (VUV) light from an H_2 discharge lamp dispersed by a 1 m normal incidence monochromator. The VUV wavelengths were calibrated using the hydrogen Lyman-α line. The ions and electrons were extracted in opposite directions with a 20 V/cm electric field. The electrons were accelerated to about 60 V into the 13 cm long velocity focusing flight tube.[34] Electrons with zero perpendicular velocity to the extraction voltage were focused to an aperture located in the center of the flight tube, whereas the energetic electrons were focused onto rings around this central spot with radii proportional to their initial perpendicular velocity to the extraction axis. They were detected by two Channeltron electron detectors. Assuming that the hot electron signal in a ring around the central spot was proportional to the hot electron contribution in the central spot, a weighted fraction of the outer ring signal is subtracted from the central electrode signal, thereby correcting the threshold electron signal for the contribution of hot electrons.[35]

The ions were accelerated to 100 eV in the 5 cm long first acceleration region and to 260 eV in a short second region. They proceeded to a 26 cm long field-free drift region and were subsequently decelerated with a −88 V ($CpMn(CO)_2CS$) and a −135 V ($CpMn(CO)_2CSe$) voltage difference. The purpose of the deceleration region is the separation of the parent ions from the fragment ions that resulted from dissociation in the 26 cm drift region. After drifting through the 8 cm long second field-free region, the ions were detected with a chevron stack of Burle multichannel plates. The electron and ion signals served as start and stop pulses for the acquisition of the ion time-of-flight (TOF) spectra. Each coincidence event was stored in an Ortec multichannel analyzer. TOF distributions were obtained in 0.5 to 12 h depending on the signal intensity and the desired spectrum quality.

The TPEPICO spectra were used for two purposes. First, the fractional abundances of the parent and the daughter ions were calculated as a function of the photon energy, which gives the breakdown diagram. Second, ion decay rates were extracted from asymmetric TOF distributions of the daughter ion signal. This asymmetry is the result of metastable ions dissociating in the 5 cm acceleration region, resulting in a time-of-flight between the parent and the daughter ion's flight time ($k <$

(17) Rue, C.; Armentrout, P. B. *J. Phys. Chem.* **2000**, *104* (21), 5046.
(18) Kretzschmar, I.; Schröder, D.; Schwarz, H.; Armentrout, P. B. *Int. J. Mass Spectrom.* **2003**, *228* (2,3), 439.
(19) Kretzschmar, I.; Schröder, D.; Schwarz, H.; Armentrout, P. B. *Int. J. Mass Spectrom.* **2006**, *249/250*, 263.
(20) Jeung G. H. *J. Am. Chem. Soc.* **1992**, *114* (9), 3211.
(21) Von Wüllen, C. *J. Chem. Phys.* **1996**, *105* (13) 5485.
(22) Dapprich, S, Pidun, U.; Ehlers, A. W.; Frenking, G. *Chem. Phys. Lett.* **1995**, *242* (4,5) 521.
(23) Saillard, J. Y.; Grandjean, D.; Caillet, P.; Le Beuze, A. *J. Organomet. Chem.* **1980**, *190*, 371.
(24) Cozak, D.; Butler, I. S.; Baibich, I. M. *J. Organomet. Chem.* **1979**, *169*, 381.
(25) Cozak, D.; Butler, I. S. *Spectrosc. Lett.* **1976**, *9* (10), 673.
(26) Butler, I. S.; Cozak, D. *Can. J. Spectrosc.* **1982**, *27* (5), 141.
(27) Barna, G. C.; Butler, I. S.; Plowman, K. R. *Can. J. Chem.* **1976**, *54* (1), 111.
(28) Butler, I. S.; Johansson, D. A. *Inorg. Chem.* **1975**, *14* (3), 701.
(29) Butler, I. S.; Xu, Z. H.; Werbowyj, R. S.; St.-Germain, F. *Appl. Spectrosc.* **1987**, *41* (1), 149.
(30) Lichtenberger, D. L.; Fenske, R. F. *Inorg. Chem.* **1976**, *15* (9), 2015.
(31) Pongor, Cs.; Gengeliczki, Zs.; Sztáray, B. *J. Organomet. Chem.*, submitted.
(32) (a) Butler, I. S.; Fenster, A. E. *Chem. Commun.* **1970**, 933. (b) Fenster, A. E.; Butler, I. S. *Can. J. Chem.* **1972**, *50*, 599. (c) Butler, I. S.; Coville, N. J.; Fenster, A. E. *Inorg. Synth.* **1973**, *16*, 53.
(33) (a) Butler, I. S.; Coville, N. J.; Fenster, E. *Inorg. Synth.* **1973**, *16*, 189. (b) Butler, I. S.; Cozac, D.; Stobart, S. R. *Chem. Commun.* **1975**, 103.
(34) Baer, T.; Li, Y. *Int. J. Mass. Spectrom.* **2002**, *219*, 381.
(35) Sztáray, B.; Baer, T. *Rev. Sci. Instrum.* **2003**, *74*, 3763.

10^3 s^{-1}). In addition, the fragment ions formed by dissociation in the first field-free region have a TOF larger than the parent ions, which we call the "drift peak". The ions that dissociate after the last acceleration region are detected as parent ions. The fractional abundances and the direct kinetic information were used together in the data analysis as described in detail in the Data Analysis section.

Quantum Chemical Calculations. The simulation of the experimental data requires vibrational frequencies and rotational constants of the equilibrium structures and transition states for the relevant neutral and ionic species. Quantum chemical calculations were performed using the Gaussian 03 package.[36] As discussed below, the lowest few frequencies of the transition states were scaled to fit the experimental dissociation rates, and therefore the accuracy of the individual transition state frequencies was not a real concern. All the calculations were carried out with the density functional theory, the B3LYP[37] exchange−correlation functional, and the 6-311G**[38] basis set. The minima of the equilibrium states were confirmed by the absence of imaginary frequencies. Various spin states were calculated for the neutral and ionic species, and the most stable ones were used to calculate the vibrational frequencies.[1] The neutral molecules were determined to be singlet, while the lowest ion energy spin multiplicities ($2S + 1$) are 2, 4, and 6 for the $CpMn(CO)_nCX^+$ ions (X = S or Se; $n = 2$, 1, and 0, respectively). In the literature, there are several works that suggest that for the dissociation of a metal−CO bond there is no reverse barrier. Experimentally, Dearden et al. found that there are no barriers for addition of CO to $Mn(CO)_x^+$ ($x = 1-5$).[39] The same was obtained for the dissociation in the $Fe(CO)_x^+$ ($x = 1-5$) system.[40] Quantum chemical calculations gave a potential energy curve without reverse barrier for the $CpCo(CO)_2$ system as well.[2] Therefore we assume that the dissociation steps of our molecules proceed with no reverse barrier. Because the dissociations proceed without a reverse barrier, the transition states do not correspond to a critical point on the potential energy surface. To approximate the structure and vibrational frequencies of the transition states, the metal−carbonyl bond distances of the leaving carbonyl group were fixed at 5 Å and the remaining coordinates were optimized. The 5 Å distance was suggested by previous works on similar compounds.[1,2] In the RRKM model, the TS frequencies were used as the starting point in the fitting of the experimental dissociation rate curves. The lowest four frequencies of the transition states, which turn into product rotations and translations, were scaled to fit the calculated TOF distributions and breakdown diagrams to the experimental ones.

One of the central results of the present TPEPICO study is the CO → CS substitution heats for the neutral complexes. To justify the derived experimental numbers, they were compared with the results of quantum chemical calculations at the B3LYP/6-311G** and G2 levels of theory. In addition to the sample complexes, calculations were performed for $CpMn(CO)_3$ and the three ligands CO, CS, and CSe as well. In all of these calculations, the zero-point vibrational energy was also taken into account.

(36) Frisch, M. J.; et al. *Gaussian 03, Revision B.04*; Gaussian, Inc.: Pittsburgh, PA, 2003.

(37) (a) Becke, A. D. *J. Chem. Phys.* **1992**, *97*, 9173. (b) Lee, C.; Yang, W.; Parr, R. G. *Phys. Rev.* **1988**, *B37*, 785.

(38) (a) Krishnan, R.; Binkley, J. S.; Seeger, R.; Pople, J. A. *J. Chem. Phys.* **1980**, *72*, 650. (b) Blaudeau, J.-P.; McGrath, M. P.; Curtiss, L. A.; Radom, L. *J. Chem. Phys.* **1997**, *107*, 5016. (c) Wachters, A. J. H. *J. Chem. Phys.* **1970,** *52*, 1033. (d) Hay, P. J. *J. Chem. Phys.* **1977**, *66*, 4377.

(39) Dearden, D. V.; Hayashibara, K.; Beauchamp, J. L.; Kirchner, N. J.; von Koppen, P. A. M.; Bowers, M. T. *J. Am. Chem. Soc.* **1989**, *111*, 2401.

(40) Schultz R. H.; Crellin K. C.; Armentrout P. B. *J. Am. Chem. Soc.* **1991**, *113*, 8590.

Results and Discussion

TOF Distributions and Breakdown Diagrams. The adiabatic ionization energies (IEs) of the complexes were obtained from the He I photoelectron spectra.[31] While the vertical IE is readily determined from the peak maximum to be 7.84 ± 0.03 and 7.86 ± 0.03 eV for the CS and CSe compounds, respectively, the adiabatic IE is difficult to extract from a broad band in the photoelectron spectrum. The adiabatic ionization energy of $CpMn(CO)_3$ is 7.69 ± 0.02 eV, determined with threshold photoelectron spectroscopy (TPES).[1] Ultraviolet photoelectron spectroscopy (UPS) gives a vertical ionization energy of 7.94 ± 0.03 eV.[31] The difference of the adiabatic and vertical ionization energies of $CpMn(CO)_3$ was used to estimate the adiabatic IEs of the CS- and CSe-substituted complexes from their vertical ionization energies. This method gives an adiabatic ionization energy of 7.59 ± 0.05 and 7.61 ± 0.05 eV, respectively. The assumption that the difference in the adiabatic and the vertical ionization energies in the chalcocarbonyl analogues can be approximated by the value for $CpMn(CO)_3$ is based on the facts that (a) the ionization is from very similar orbitals in these complexes and (b) the vibrational structure in the three complexes is almost identical, so that the Franck−Condon factors should be similar and result in a similar vibrational envelope.

TOF mass spectra of both compounds were collected in the photon energy range of 8.3−13.5 eV. Three sequential dissociation reactions associated with the loss of CO, CO, and CX are observed for both compounds. The spectra at low energies correspond to the loss of the first CO group. At higher energies, the CO loss fragment ion becomes the parent ion for the next CO loss reaction. Finally, at still higher energies, the $CpMnCX^+$ ion loses the CX ligand. In the TOF spectra of the selenium complex, the peaks can be assigned analogously.

Figure 1a,b shows the breakdown diagram of $CpMn(CO)_2CS^+$ and $CpMn(CO)_2CSe^+$. The ion fractional abundance is plotted as a function of the photon energy. The points are the experimental ratios, the solid lines show the result of the RRKM simulations, and the arrows indicate the location of the three 0 K appearance energies. (Throughout the text, we refer to the 0 K energy difference between a daughter ion and the neutral parent molecule as the appearance energy. This is not equal to the visual experimental appearance energy, which includes kinetic and thermal shifts.) In the first photodissociation reaction, $CpMn(CO)_2CX^+ \rightarrow CpMn(CO)CX^+ + CO$, the crossover in the breakdown of the parent ion is quite steep, indicating a narrow distribution of the ion internal energy. The second and the third crossovers, corresponding to the carbonyl loss from $CpMn(CO)CX^+$ and to the thio- and selenocarbonyl loss from $CpMnCX^+$, are increasingly wider, indicating wider distributions of the ion internal energies.

The sequential dissociation reaction mechanism of the $CpMn(CO)_2CX^+$ ions are described by eq 1.

$$CpMn(CO)_2CX^+ \rightarrow CpMn(CO)CX^+ + CO \rightarrow CpMnCX^+ + 2CO \rightarrow CpMn^+ + 2CO + CX \quad (1)$$

The appearance energies of the first and the second CO loss are very close (see Figure 1); that is, the $CpMn(CO)CS^+$ ion is stable only in a small energy range and readily dissociates to $CpMnCS^+ + CO$, which explains the weak $CpMn(CO)CS^+$ ion

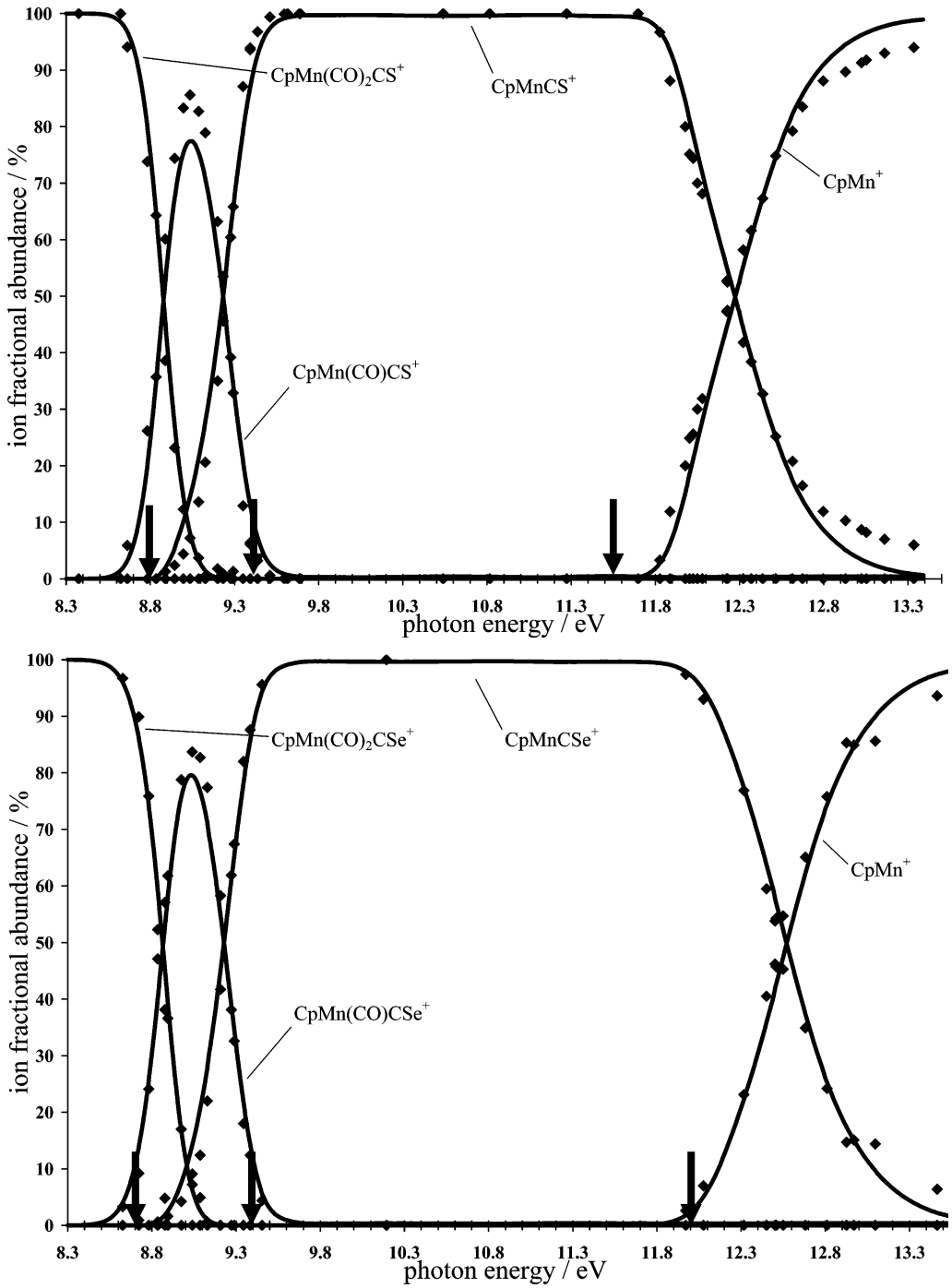

Figure 1. Breakdown curves of the three dissociation steps. The dots are the experimental data, the solid lines are the results of the RRKM simulations, and the arrows indicate the location of the three 0 K dissociation appearance energies.

signal in the electron ionization experiments, where the energy resolution is rather poor.[14]

The product ion TOF distributions are asymmetric at energies close to the appearance energies. This indicates that the ions dissociate while traveling in the first acceleration region of the ion optics. If the average lifetime of the ions is comparable to the time it takes to traverse the acceleration regions, the time-of-flight of the fragment ion is between the precursor and product ion TOF, and a quasi-exponential shape is observed in the product ion peak. The decay rate can be extracted from the analysis of the peak shapes.

Data Analysis. The thermal energy distribution of the molecular ion, $CpMn(CO)_2CX^+$, is much wider than the TPEPICO resolution (about 12 meV). Thus, it is necessary to interpret the measured rate constants in terms of a distribution of $k(E)$, in which the energy extends over the thermal energy distribution to obtain a proper RRKM fit to the experimental data on the three consecutive dissociation reactions in eq 1.

The first step of the analysis is the calculation of the thermal energy distribution of the neutral molecules in which we use the density of ro-vibrational states calculated by the direct count method.[41] The harmonic frequencies and rotational constants were determined by quantum chemical calculations as discussed above. The lowest frequency mode, namely, the cyclopentadienyl ring rotation, was treated as a hindered (Pitzer) rotor.[41,42]

(41) Baer, T.; Hase, W. L. *Unimolecular Reaction Dynamics: Theory and Experiments*; Oxford University Press: New York, 1996.

(42) Pitzer, K. S. *Quantum Chemistry*; Prentice Hall: New York, 1953.

The moment of inertia of the hindered rotor and the cyclopentadienyl ring was obtained from the calculated structure of the equilibrium states, while for the barrier height a value used in earlier studies on manganese complexes was employed.[1,5]

The energy distribution of the molecular ion is obtained as the convolution of the energy resolution function with the energy distribution of the neutral minus the adiabatic IE. The product energy distribution for both the daughter ion and the leaving neutral fragment needs to be taken into account for subsequent photodissociation reactions. After the parent ions of a particular internal energy, E, dissociate, they leave behind daughter ions in a distribution of internal energies from 0 to $E - E_0$, where E_0 is the dissociation barrier. The 0 means that all the excess energy was taken away by the leaving CO molecule, while in the latter case all the energy remains in the fragment ion. The probability that E_i energy remains with the daughter ion can be derived statistically by the following equation:

$$P(E_i, E - E_0) \propto \rho_{\text{daughter}}(E_i)\rho_{\text{rv,t,ligand}}(E - E_0 - E_i) \quad (2)$$

where $\rho_{\text{rv,t,ligand}}$ is the rovibrational and relative translational density of state of the departing CO ligand.

The RRKM theory was used to calculate the unimolecular rate constants of the various sequential dissociation reactions. The rate constant is given by the well-known formula[41]

$$k(E) = \frac{\sigma N^{\ddagger}(E - E_0)}{h\rho(E)}, \quad (3)$$

in which $N^{\ddagger}(E - E_0)$ is the sum of states of the transition states at $E - E_0$, and $\rho(E)$ is the density of states of the ion measured from the bottom of the ion ground state potential energy well. The symmetry parameter, σ, is 2, 1, and 1 in the three dissociation steps, respectively.

The ion TOF distributions and the breakdown diagrams can be calculated using the thermal energy distribution of the neutral $CpMn(CO)_2CX$ molecules, the internal energy distribution of the dissociating ions, the ionization energies, the ion optics parameters, and the transition state vibrational frequencies. The dissociation limits and the lowest four TS vibrational frequencies were adjusted until the best fit was obtained.

The following appearance energies were thus determined in the fit for $CpMn(CO)CS^+$, $CpMnCS^+$, $CpMn^+$, $CpMn(CO)CSe^+$, $CpMnCSe^+$, and $CpMn^+$: 8.79, 9.42, 11.53, 8.70, 9.39, and 12.05 eV, respectively. All appearance energy values have an uncertainty of 0.05 eV, as discussed below. In the first approximation, each appearance energy is independent of the previous ones because we always start from the neutral parent molecule so that the error bars do not increase with subsequent photodissociation steps. The simulated breakdown diagrams are shown in Figure 1a,b.

The uncertainties for the appearance energies were determined by testing the sensitivity of the fit to the assumed vibrational frequencies by fixing the lowest four transition state frequencies at various values and carrying out the fitting procedure. This scheme simulates looser and tighter transition states, thereby altering the $k(E)$ rate curves. It was found that changing the lowest four frequencies by ± 50% did not affect the simulated breakdown diagram significantly, but the quality of the TOF distributions got significantly worse. This is because the quasi-exponential shape of the asymmetric daughter ion distributions depends on the absolute dissociation rate, whereas the breakdown diagram depends only on the ratio of the rate constants. The optimized appearance energies change by ±0.05 eV, with the altered transition state frequencies, which suggests an error bar of ±0.05 eV for these parameters.

From the appearance energies and ionization energies we could obtain the bond energies:

$$D_1 = \text{AE}[\text{CpMn(CO)CX}^+] - \text{IE}[\text{CpMn(CO)}_2\text{CX}]$$

$$D_2 = \text{AE}[\text{CpMnCX}^+] - \text{AE}[\text{CpMn(CO)CX}^+]$$

$$D_3 = \text{AE}[\text{CpMn}^+] - \text{AE}[\text{CpMnCX}^+]$$

From the error bars of ionization energies and appearance energies we estimated the error limits of bond energies (D_{1-3}) to be 0.06, 0.07, and 0.07 eV for D_1, D_2, and D_3, respectively. The 0 K bond energies for the consecutive dissociation reactions are 1.20 ± 0.06, 0.63 ± 0.07, 2.12 ± 0.07 and 1.08 ± 0.06, 0.72 ± 0.07, 2.66 ± 0.07 eV for the three dissociation steps of $CpMn(CO)_2CS$ and $CpMn(CO)_2CSe$, respectively.

The dissociation appearance energies for the first CO loss and the CX loss are lower than the crossover energies for both compounds, while the second dissociation appearance energy is slightly higher than its crossover energy. The ideal 0 K breakdown curve with infinitely rapid dissociation steps would exhibit sharp steps (down for the precursor ion and up to the fragment ion) at the dissociation appearance energy. As discussed in detail by Sztáray and Baer,[2] the experimentally measured breakdown curve shows the effect of thermal energy distribution of the sample and the kinetic shift of slow reaction. The thermal energy shifts the crossover energy to a lower energy, while the kinetic shift moves the crossover energy to a higher energy. The rate constant for the first CO loss increases slowly, which results in a large kinetic shift. On the other hand, the low activation energy for the second CO loss step results in a rapid dissociation so that the kinetic shift is negligible, and the 0 K appearance energy of the $CpMnCS^+$ ion is located somewhat to the right of the crossover energy. The loss of the final CX group is associated with a slower rate constant, and a significant amount of the energy is lost as translational and rotational energy of the two leaving CO molecules; therefore the 0 K appearance energy is again well below the crossover energy.

The activation entropies of the three consecutive dissociation reactions are 41.5, 63.1, 38.1 and 14.9, 40.8, 24.3 J/(K mol) at 600 K for X = S and Se, which indicates that these reactions proceed via loose transition states, as is characteristic of simple bond-breaking reactions.

Thermochemical Data. In order to convert the appearance energies into heats of formation, we use the high-energy product ion $CpMn^+$ as an anchor for the heat of formation scale. The heat of formation of this ion was determined in a previous study on the Cp_2Mn system.[5] Thus, the appearance energy for the $CpMn(CO)_2CX + h\nu \rightarrow CpMn^+ + 2CO + CX$ reaction, together with the heats of formation of the CO and CX molecules, yields the heat of formation of the $CpMn(CO)_2CX$ molecule. Although the heat of formation of CO is listed with great precision in all compilations, the same does not apply for the heat of formation of CS, which is listed by Wagman et al.[43] as 230 kJ/mol and by Chase[44] as 277 ± 25 kJ/mol, although Okabe[45] measured the appearance energy of the CS A-X fluorescence and, thus, obtained the bond energy in the ground

(43) Wagman, D. D.; Evans, W. H. E.; Parker, V. B.; Schum, R. H.; Halow, I.; Mailey, S. M.; Churney, K. L.; Nuttal, R. L. *The NBS Tables of Chemical Thermodynamic Properties*; *J. Phys. Chem. Ref. Data*, Vol. 11, Suppl 2: NSRDS, U.S. Government Printing Office: Washington DC, 1982; p 1.

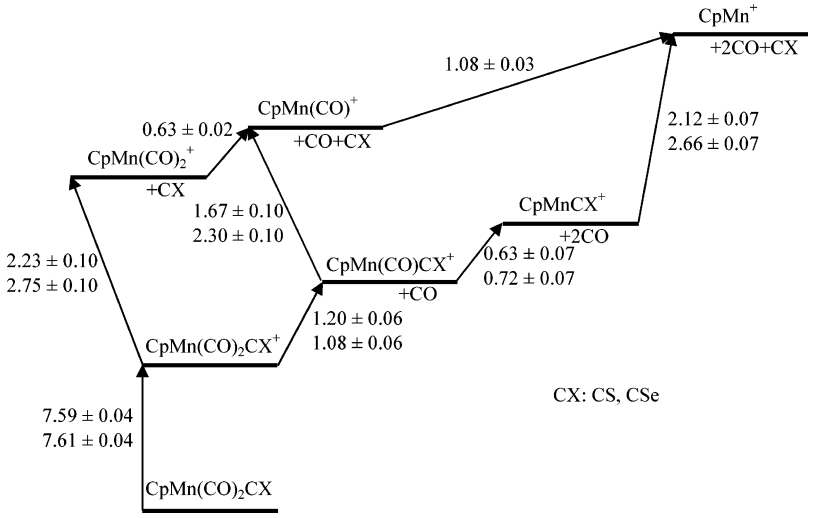

Figure 2. Thermochemistry of the $CpMn(CO)_2CX$ (X = S, Se) systems. Ionization energies and bond energies are indicated in eV with their uncertainties. Values for the X = S system are listed above those for the X = Se system.

Table 1. Auxiliary and Derived Thermochemical Data (bond energies in eV, heats of formations in kJ mol^{-1})

	$D_0(Mn^+-CO)$	$D_0(Mn^+-CX)$	$\Delta_fH_{0K}°$	$\Delta_fH_{298K}°$	$H_{298K}° - H_{0K}°$
CO			-113.8 ± 0.2[a]	-110.5 ± 0.2[a]	8.7[b]
CS			271.8 ± 1.7[c]	275.0 ± 1.7[d]	8.7[b]
CSe			367.4 ± 5.9[e]	366.3 ± 5.9[d]	6.2[b]
$CpMn^+$			947 ± 16[f]	935 ± 16[f]	19.5[f]
$CpMn(CO)_3$		1.11 ± 0.04[f]	-408 ± 17[f]	-424 ± 17[f]	31.9[f]
$CpMn(CO)_2CS$			-122 ± 17[g]	-137 ± 17[d]	32.4[b]
$CpMn(CO)_2CSe$			-76 ± 18[g]	-92 ± 18[d]	33.0[b]
$CpMn(CO)_2CS^+$	1.20 ± 0.06[g]	2.23 ± 0.10[g]	611 ± 17[g]	597 ± 17[d]	34.1[b]
$CpMn(CO)_2CSe^+$	1.08 ± 0.06[g]	2.75 ± 0.10[g]	656 ± 18[g]	642 ± 18[d]	34.7[b]
$CpMn(CO)CS^+$	0.63 ± 0.07[g]	1.67 ± 0.10[g]	840 ± 17[g]	827 ± 17[d]	29.4[b]
$CpMn(CO)CSe^+$	0.72 ± 0.07[g]	2.30 ± 0.10[g]	875 ± 18[g]	861 ± 18[d]	29.9[b]
$CpMnCS^+$		2.12 ± 0.07[g]	1014 ± 17[g]	1012 ± 17[d]	24.7[b]
$CpMnCSe^+$		2.66 ± 0.07[g]	1058 ± 18[g]	1045 ± 18[d]	25.1[b]

[a] CODATA key values for thermodynamics.[46] [b] Determined from the DFT calculated vibrational frequencies. [c] $\Delta_fH°_{0K}[CS_2] + D_0[CS_2] - \Delta_fH°_{0K}[S]$. [d] $\Delta_fH°_{0K} \rightarrow \Delta_fH°_{298K}$. [e] $\Delta_fH°_{0K}[C] + \Delta_fH°_{0K}[Se] - D_0[CSe]$. [f] Li et al.[1,5] [g] This study.

Table 2. Reaction Enthalpies Derived from the Heats of Formations (in kJ mol^{-1})

	$\Delta_rH_{0K}°$			$\Delta_rH_{298K}°$
reaction	B3LYP/6-311G**	G2		experimental
$CpMn(CO)_3 + CS \rightarrow CpMn(CO)_2CS + CO$	-87.5	-70.3	-99 ± 8	-99 ± 8
$CpMn(CO)_3 + CSe \rightarrow CpMn(CO)_2CSe + CO$	-98.6	-94.6	-149 ± 8	-145 ± 8

state of CS_2, 430.6 ± 1.3 kJ/mol. This, combined with the heat of formation of $\Delta_fH°_{0K}[CS_2] = 116.9 \pm 0.8$ kJ/mol[44] and the $\Delta_fH°_{0K}[S] = 277.17 \pm 0.15$ kJ/mol,[46] yields $\Delta_fH°_{0K}[CS] = 270.4 \pm 1.5$ kJ/mol.

Smoes and Drowart measured a C−Se bond dissociation energy of 586.6 ± 5.6 kJ/mol from equilibrium measurements using the Knudsen cell method.[47] This bond energy is confirmed by calculations of Deakyne et al.[48] The heat of formation of the CSe molecule can thus be established with the help of the heat of formation of the Se atom, which is listed as 237.3 ± 0.6 kJ/mol by Smoes[47] and 226.4 by Wagman et al.[49] The latter value, however, seems to be referring to a list prepared in 1964, so we used the more recent Smoes's value. This, with the heat of formation of $\Delta_fH°_{0K}[C] = 716.68 \pm 0.45$ kJ/mol,[50] gives $\Delta_fH°_{0K}[CSe] = 367.4 \pm 5.9$ kJ/mol.

The molecular ions' heats of formation can also be obtained from the derived heats of formation of the neutral molecules and their adiabatic ionization energies. By combining the neutral heats of formation with the $CpMn(CO)CX^+$ appearance energies, the 0 K heats of formation of $CpMn(CO)CX^+$ can be obtained. In a similar way, the heats of formation of $CpMnCX^+$ can also be determined. The derived thermochemical data are shown in Table 1.

Although, experimentally only the Mn−CO bond breaking can be observed in the first two steps of the TPEPICO experiments, one can also get the Mn−CX bond energies in each dissociating ion. For this the heats of formation derived above are to be combined with the heats of formation of the $CpMn(CO)_n^+$ (n = 2, 1, 0) species, determined in an earlier study[1] and later revised due to a more precise $CpMn^+$ heat of

(44) Chase, M. W., Jr. *NIST-JANAF Thermochemical Tables*, 4th ed.; *J. Phys. Chem. Ref. Data, Monogr.* 1998; pp 1−1951.
(45) Okabe, H. *J. Chem. Phys.* **1972**, *56*, 4381.
(46) Cox, J. D.; Wagman, D. D.; Medvedev, V.A. *CODATA Key Values for Thermodynamics*; Hemisphere Publishing Corp.: New York, 1984.
(47) Smoes, S.; Drowart, J. *J. Chem. Soc.* **1977**, *73* (12), 1746.
(48) Deakyne, C. A.; Li, L.; Zheng, W.; Xu, D.; Liebman, J. F. *J. Chem. Thermodyn.* **2002**, *34*, 185.
(49) Wagman, D. D.; Evans, W. H. E.; Parker, V. B.; Schum, R. H.; Halow, I.; Mailey, S. M.; Churney, K. L.; Nuttal, R. L. *The NBS Tables of Chemical Thermodynamic Properties*; *J. Phys. Chem. Ref. Data*, Vol. 11, Suppl 2: NSRDS, U.S. Government Printing Office: Washington DC, 1982; p 1.
(50) Cox, J. D.; Wagman, D. D.; Medvedev, V. A. *CODATA Key Values for Thermodynamics*; Hemisphere Publishing Corp.: New York, 1984.

formation.[5] Figure 2 shows the 0 K thermochemistry of the $CpMn(CO)_2CX$ system, and the derived bond energies are listed in Table 1. It can be seen that in both of our compounds, the Mn−CX bond is significantly stronger than the Mn−CO bond: the Mn−CX (CX = S, Se) bond energies are larger than the Mn−CO bond energies by 1.04 and 1.61 eV on the average. This agrees well with the general observation that the CX ligand is more strongly bound to the metal center than the carbonyl ligand in transition metal organometallic complexes[11−14] and also with the lack of CX loss from $CpMn(CO)_2CX^+$ and $CpMn(CO)CX^+$ in our experiment.

In order to convert the derived 0 K enthalpies to 298 K values, we calculated the thermal energy function, $H_{298K}° - H_{0K}°$, for the various species using the B3LYP/6-311G**-calculated vibrational frequencies. In the thermal contribution of the lowest frequency (Cp-ring rotation) a rotational degree of freedom was used instead of a harmonic vibration. Using these data with the $H_{298K}° - H_{0K}°$ values of the elements (C, 1.051 kJ/mol; H_2, 8.467 kJ/mol; Mn, 4.994 kJ/mol; O_2, 8.683 kJ/mol; S, 4.412 kJ/mol; Se, 6.199 kJ/mol),[50,51] we calculated the room-temperature heats of formation of the $CpMn(CO)_2CX$ molecules and the ionic species as listed in Table 1. Throughout these calculations, the Rosenstock (ion) convention[52] was used, in which the heat of capacity of the electron was treated as 0.0 kJ/mol at all temperatures.

The bond energies in Figure 2 refer to the ionic species. However, bond energies in neutral species are of more interest to organometallic chemists. Although the absolute values of the neutral bond energies cannot be determined from the present work without the ionization energies of the unstable [M−CO] molecules, using the appearance energy of $CpMn^+$ from $CpMn(CO)_3$ determined in an earlier[1,5] study and the appearance energy of $CpMn^+$ from $CpMn(CO)_2CX$ we can obtain the reaction enthalpies for the following reactions:

$$CpMn(CO)_3 + CX \rightarrow CpMn(CO)_2CX + CO \qquad (6)$$

$\Delta_r H_{0K}° = -99 \pm 8$ kJ/mol and -149 ± 8 kJ/mol for X = S and Se, respectively. It is important to point out that, since the reaction enthalpies are determined as the difference of two appearance energies, the error bars of these enthalpies depend only on the errors of the appearance energies. The room-temperature substitution heat was derived to be $\Delta_r H_{298K}° = -99 \pm 8$ kJ/mol and -145 ± 8 kJ/mol for X = S and Se, respectively (Table 2). The substitution heats, which in fact are the differences in the Mn−CO and Mn−CX bond energies, appear to be quite exothermic, in accordance with the fact that the CX ligands are bonded stronger to the transition metal center than the CO ligand. In order to give a computational justification for these quite significant stabilizations, the substitution heats were calculated at the B3LYP/6-311G** and the G2 levels of theory. In the DFT calculations, ZPE corrections were done using the unscaled harmonic frequencies. As can be seen in Table 2, the calculated values differ significantly from the experimental values, but these calculated numbers cannot be expected to be precise, only their magnitude should be considered. On this basis, the calculations seem to support the surprisingly large bond enthalpy differences.

From Figure 2, it can be deduced that the carbonyl replacement with chalcocarbonyls has a slight effect on the Mn−CO dissociation energy. Exchanging one carbonyl ligand for thiocarbonyl or selenocarbonyl marginally destabilizes the manganese−carbonyl bond by approximately 3 and 12 kJ/mol, respectively. Consequently, the CO → CX change should have a minor influence on the catalytic activity of the $CpMn(CO)_3$, and transition metal carbonyls in general; however it causes a significant stabilization of the complex. This might mean that the conditions in which these transition metal complexes can be utilized can be extended by carbonyl replacement with chalcocarbonyls.

Conclusions

Threshold photoelectron photoion coincidence spectroscopy has been used to investigate the dissociation kinetics of the $CpMn(CO)_2CX^+$ (X = S, Se) ions. The dissociation of the $CpMn(CO)_2CX^+$ ion proceeds by the sequential loss of CO and CX molecules. By fitting the metastable ion time-of-flight distributions and the breakdown diagrams with the statistical RRKM theory, accurate 0 K appearance energies were obtained for the fragment ions $CpMn(CO)_n(CX)_m^+$ ($n = 2, 1, 0$; $m = 1, 0$). Combined with the ionization energy of $CpMn(CO)_2CX$, the ion bond energies for the two Mn−CO bonds and the Mn−CX bond were determined. Using the known heats of formation of the products ($CpMn^+$, CO, CX), the heats of formation of the $CpMn(CO)_n(CX)_m^+$ ($n = 2, 1, 0$; $m = 1, 0$) ions and the $CpMn(CO)_2CX$ molecules were calculated.

The derived Mn−CX bond energies in the various ionic species show that CX ligands are always more strongly bonded to the transition metal center than the CO ligand. This is in accordance with the better σ-donor and π-acceptor properties of the CX ligands.[53−56] Combining the determined heats of formation with the heats of formation of the $CpMn(CO)_3$ from an earlier TPEPICO study and with that of the fragment ions, we obtained the substitution enthalpy of the carbonyl replacement with the CS and CSe ligands. $CpMn(CO)_2CS$ is more stable than $CpMn(CO)_3$, and the formation of $CpMn(CO)_2CSe$ is even more favored thermodynamically than the formation of the CS derivative.

Acknowledgment. We are grateful to the U.S. Department of Energy for financial support as well as to the International Office of the U.S. National Science Foundation and the Hungarian Academy of Science for a joint U.S.−Hungary grant. We are also grateful to the Hungarian National Science Fund (grants no. OTKA F61153 and T032489) for supporting this work. The help of Dávid Frigyes with the mass spectrometry and of Gábor Magyarfalvi and György Tarczay with the IR spectra is acknowledged.

OM060379J

(51) Chase, M. W., Jr. *NIST-JANAF Thermochemical Tables*, 4th ed.; *J. Phys. Chem. Ref. Data, Monogr*. 1998; pp 1−1951.

(52) Rosenstock, H. M.; Draxl, K.; Steiner, B. W.; Herron, J. T. Energetics of gaseous ions. *J. Phys. Chem. Ref. Data*, Vol. 6, American Chemical Society: Washington DC, 1977.

(53) Broadhurst, P. V. *Polyhedron* **1985**, *4*, 1801.

(54) Cozak, D.; Butler, I. S.; Baibich, I. M. *J. Organomet. Chem.* **1979**, *169*, 381.

(55) Bodner, G. M. *Inorg. Chem.* **1974**, *13*, 2563.

(56) Hickey, J. P.; Baibich, I. M.; Butler, I. S.; Todd, L. *J. Spectrosc. Lett.* **1978**, *11*, 671.